Available online at www.sciencedirect.com

ScienceDirect

Energy Procedia 69 (2015) 769 – 778

Energy Procedia

International Conference on Concentrating Solar Power and Chemical Energy Systems, SolarPACES 2014

Experiments on a lab scale TES unit using eutectic metal alloy as PCM

P. Blanco-Rodríguez[a]*, J. Rodríguez-Aseguinolaza[a], A. Gil[a], E. Risueño[a], B. D'Aguanno[a], I. Loroño[b], L. Martín[c]

[a]*CIC Energigune, c/ Albert Einstein 48, 01510-Miñano (Álava), Spain*
[b]*Dept. ciencias y técnicas de la navegación, máquinas y construcciones navales, Escuela técnica superior de náutica y máquinas navales, UPV-EHU, 48920-Portugalete (Vizcaya), Spain*
[c]*Dept. máquinas y motores térmicos, Escuela técnica superior de ingeniería, UPV-EHU, 48013-Bilbao (Vizcaya), Spain*

Abstract

The behavior of a magnesium and zinc eutectic metal alloy used as thermal energy storage (TES) material is tested in a laboratory scale TES unit. The TES unit consists of two concentric tubes with the central tube surrounded by 67 kg of the metal alloy and two caps at both ends of the tube through which the heat transfer fluid (HTF) flows. Charging (melting) and discharging (solidification) processes of the eutectic metal alloy are performed using synthetic oil as the HTF. The experimental results are used to test the validity of the model via simulations performed with a computational fluid dynamics tool.
The results corroborate that phase change materials with high thermal conductivity, such as eutectic metal alloys, are ideal for the evaporation process of water in direct steam generation applications due to the quasi-constant melting and solidification temperatures and to its high heat transfer capacity.

Peer review by the scientific conference committee of SolarPACES 2014 under responsibility of PSE AG

Keywords: Latent heat storage; phase change material; eutectic alloy; direct steam generation; concentrated solar power

* Corresponding author. Tel.: +34-945-297-108;
E-mail address: pblanco@cicenergigune.com

Peer review by the scientific conference committee of SolarPACES 2014 under responsibility of PSE AG
doi:10.1016/j.egypro.2015.03.087

1. Introduction

The deployment of direct steam generation concentrated solar power (DSG-CSP) plants depends strongly on suitable thermal energy storage (TES) systems. Current commercial DSG-CSP plants store steam allowing just one extra hour operation of the power block, which seems to be a short time compared with other CSP technologies that use the well-known two tank molten salt technology. Notwithstanding in the last years a big research effort has been done in order to find an appropriate TES system for DSG by means of using phase change materials (PCM) [1–4], there is no commercial CSP plant running with such a system yet. All these approaches [1–4] employ molten salts as PCM. It is well known that the main drawback of the molten salts is their low thermal conductivity which leads to the use of sophisticated heat exchangers. In order to overcome this drawback, the idea of using eutectic metal alloys has been returned [5, 6].

The objective of this study is to demonstrate the viability of eutectic metal alloys as TES materials. A systematic set of experiments has been performed in a laboratory scale TES unit highlighting the benefits of using PCMs with high thermal conductivity. In addition, the study has been validated by CFD simulations.

Nomenclature

H	enthalpy function	ρ	density
$\vec{v}$	liquid velocity	β	liquid volume fraction
A_{mush}	mushy zone constant	$\vec{v}_p$	solid velocity
S	source term	κ	thermal conductivity
M_S	momentum sink	Re	Reynolds number

2. Prototype and model description

2.1. Oil test loop

Although the main proposed application of the studied material is for DSG and therefore water should be used as the HTF, oil has been used instead because of the ease of the installation at the laboratory scale. The oil test loop has 40 kW power provided by low density ($2W/cm^2$) electrical heaters. It has a magnetic circulation pump (Dickow) with a pumping capacity of 25 m3/h and a 90 kW air fan heat exchanger for cooling process. The piping system is of 2 inches diameter. The design pressure of the installation is 20 bar and the maximum working temperature is limited to 400 ºC due to the use of Syltherm 800 heat transfer fluid (HTF).

The oil flow is measured by an ultrasound flowmeter (UFM 530, Krone). An automatic three-way-valve controls the oil flow directed to the TES unit from 5 ± 0.5 m3/h to 25 ± 0.1 m3/h. The rest of the flow is sent to the inlet of the pump by means of a bypass. A second automatic three-way-valve is used to control the temperature of the oil, especially in discharging process when the oil has to be cooled down through the air fan heat exchanger. Flow direction can be modified by means of another two automatic three-way-valves. The charging (melting) is always applied with the oil flow from top to bottom, and the contrary in the discharge (solidification), from bottom to top.

2.2. TES unit

Prior to the construction of the TES unit, a compatibility study between different container materials (SS304, SS304L, SS316 and SS316L) and the eutectic metal alloy has been performed in order to avoid undesired chemical reactions or progressive degradation of the PCM and construction materials. None of the studied stainless steels has suffered any reaction or corrosion with the eutectic alloy. Therefore, the material construction has been adopted on an economic basis, and SS304 has been finally selected for the construction of all components of the TES unit.

The TES unit consists of two concentric cylinders of one inch diameter for internal pipe and 8 inches diameter for external pipe. In between, 67 kg of Mg-51%Zn eutectic binary alloy have been placed, having thus 2.88 kWh of

energy in the phase change. The thermophysical properties of interest for TES applications have been previously determined and studied [5, 6].

The design of the unit allows to exchange the eutectic metal alloy by other materials of interest in future studies. For this reason, two caps on top and bottom ends have been placed. Moreover, the TES unit has been designed with the possibility to vary the internal pipe diameter and it allows to study the effect of the top and bottom flanges that enclose the storage material. There is free space on top of the PCM for expansion and volume change of liquid/solid phases of the alloy. This space is filled by Ar gas with an overpressure of 0.5 bars in order to avoid metal oxidation.

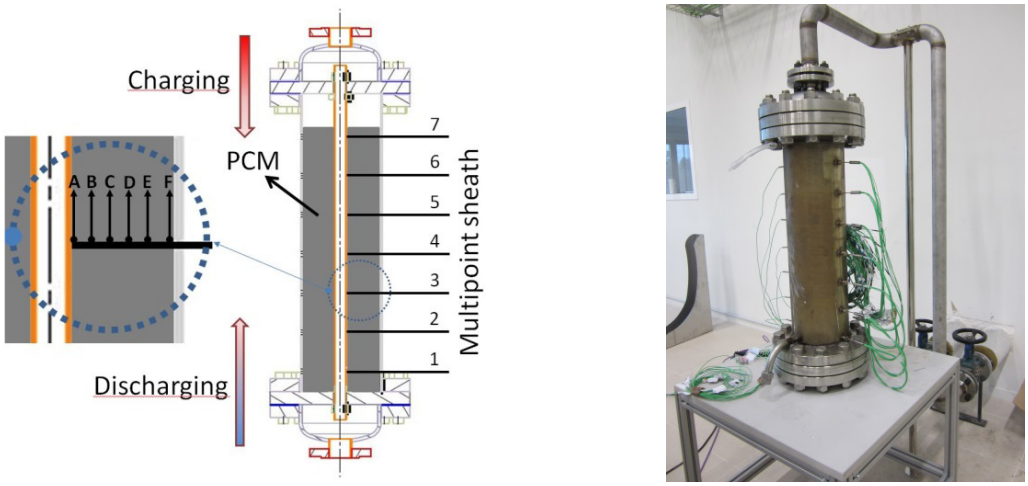

Fig. 1. (a) Scheme of the TES unit with sheath and thermocouple distribution; (b) Picture of the TES unit .

The HTF flows through the inner pipe and exchanges the heat with the surrounding metal alloy. In the charging process (melting) the oil enters from the top and exits from the bottom. In the discharging process (solidification) the oil flow is reversed, it enters from the bottom and exits from the top.

In order to register the evolution of the temperature distribution in the total volume of TES unit, seven multipoint sheaths (labeled as 1 to 7 in figure 1a) have been placed in the axial direction with six K-type thermocouples each (labeled as A to F in figure 1a) equidistantly separated in the radial direction. Additionally, two thermocouples have been placed on top and bottom flange connections in order to determine inlet temperature in both charging and discharging processes. Sheath 7 has been placed on top of the free surface of the PCM. The rest of sheaths have been dipped into the metal.

With the aim of reducing thermal losses a rock wool blanket of 0.12 m thickness has been employed to cover the entire unit. In some critical zones a second insulation layer of the rock wool blanket has been applied in order to minimize thermal losses. Fig. 1b shows a picture of the TES unit before covering it with the insulation material.

2.3. Model description

From the mathematical point of view, the phase change is a transient, nonlinear and, regarding the solid-liquid interface, a “moving boundary” problem. Due to this complexity, analytical solutions are only possible for simple and highly symmetric systems. In general, an approached frame is necessary in order to obtain accurate enough solutions for real application latent heat storage devices. Within this frame, fixed grid methods are the most accepted alternative as they provide high accuracy and do not require any tracking of the liquid/solid moving interface.

The solid/liquid fraction of the PCM can be determined by means of different approaches such as enthalpy methods and temperature based equivalent heat capacity methods. The first alternative is the most widely used one [7-9] and has been validated in a wide variety of metallurgical problems such as melting/solidification of pure metals and alloys, casting processes and others [10].

In this model two separate zones are identified. On the one hand, the PCM (Mg-Zn eutectic alloy) where the heat transfer mechanisms will be dominated by conduction in the solid phase and the solidification process and, by conduction-convection events in the melting process. However, taking into account the particular arrangement of the studied laboratory scale TES unit, where the measured temperature differences are small in the axial and radial directions and the high thermal conductivity of the solid and liquid metal alloy, the contribution of the convective heat transfer might be limited. In any case, although the quantification of this contribution needs further investigations, both convective and conductive heat transfer phenomena are included in the performed calculation. For this zone, the energy equation solved in this method is:

$$\frac{\partial(\rho H)}{\partial t} + \nabla \cdot (\rho \vec{v} H) = \nabla \cdot (\kappa \nabla T) + S \tag{1}$$

where H is the enthalpy function, ρ the density of the PCM, $\vec{v}$ the velocity of the liquid, κ the thermal conductivity and S a generic source term, zero in our simulations. In this enthalpy-porosity formulation of the phase change problem, the momentum sink (M_s) introduced to describe the melting/solidification process is given by:

$$M_S = \frac{(1-\beta)^2}{(\beta^3 + \varepsilon)} A_{mush} (\vec{v} - \vec{v}_p) \tag{2}$$

where β is the liquid volume fraction, ε is a small number fixed to 0.001 to prevent division by zero, A_{mush} is the mushy zone constant and $\vec{v}_p$ is the solid velocity due to the pulling velocity of solidified material out of the domain, zero in our simulations.

The mushy zone constant (A_{mush}) represents the amplitude of the damping between both phases [11, 12], modeled as a porous zone. High values imply steeper transition of the velocity from the liquid to the solid values. However, even for isothermal transformations like eutectic phase changes, this value cannot be very large as it might cause the solution to oscillate. In our case a value of A_{mush}=100000 has led to satisfactory values.

On the other hand, the calculation of the liquid fraction (β) in this method is based on the porous media formulation of the melting process. In particular, the porosity value ranges from ε=0 to ε=1 from the solid to liquid phase, which leads to a liquid fraction ranging from β=0 to β=1, respectively. For intermediate values, taking into account the eutectic and hence isothermal transition behavior of the modeled PCM, an iterative process between the energy equation and the liquid fraction described in [13] has been used. In the simulations, no volume change between solid and liquid phases of the PCM has been taken into consideration.

In the HTF zone the governing heat transfer mechanisms will correspond to convective processes. The HTF was always in turbulent flow (Re>40000). In this case, a standard k-ε Reynolds Average Navier Stokes model [14, 15] has been used in order to model the fluid dynamics. The main assumptions of the model are the following:

- Isotropic and homogeneous phase change material.
- Incompressible and Newtonian fluids.
- Constant heat transfer fluid inlet temperature and velocity.
- 2-D axisymmetric model.
- No viscous dissipation.

The complete calculation has been performed by using Ansys Fluent® commercial computational fluid dynamics (CFD) software with a successful compromise between the accuracy, convergence and time requirements.

3. Results and Discussion

3.1. Melting and solidification of metal PCM

As one of the goals of this work is to study how the eutectic alloy behaves in melting and solidification processes, as an example Fig. 2 shows the temperature profile of the six thermocouples of sheath 4. Prior to the beginning of the experiment the system was equilibrated to around 305 ºC. Then, for the melting test, the oil inlet temperature has been set to 381 ºC with an oil velocity of 1 m/s. For the solidification test, the HTF inlet temperature has been set to 306 ºC with same oil velocity. In the heating, three different regions can be easily distinguished:

- The first one corresponds to the preheating of the solid alloy where the temperature of the alloy is gradually increased up to the melting point.
- The second one corresponds mainly to the melting process that occurs at a temperature of 342 ºC. This temperature agrees with the values obtained in previous calorimetric experiments [5, 6].
- The last one is the superheating of the liquid melt to the set value of 381 ºC. It has to be stressed that during the melting, there is some preheating and superheating of the alloy as well.

In the cooling process a similar behavior is observed:

- First, the cooling of the liquid melt.
- Then the solidification at a quasi-constant temperature.
- Finally the cooling of the solid phase up to the inlet HTF temperature.

In the heating process, it is considered that the melting starts when the first thermocouple (always A) reaches the melting point. The melting process ends when last thermocouple (always F) overpasses the melting point. For consistency, the inflection point of the temperature curve has been taken. Similar criterion has been used for the cooling process.

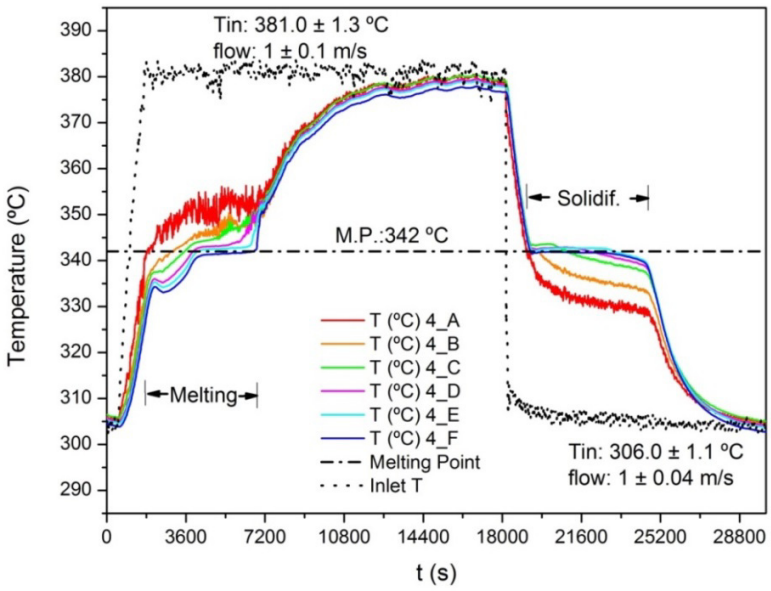

Fig. 2. Temperature evolution of thermocouples of sheath 4 in melting and solidification processes.

Once the melting process starts, the heating rate of all thermocouples is drastically reduced. The temperature profile of thermocouple 4A is flattened and remains at quasi-constant temperature above the melting point and below the set value until all PCM at that level is melted. After the melting, the heating rate speeds up again until it approaches the set value. During the melting, the temperature difference between 4A and melting point is $\Delta T < 10$ºC. This is the one needed to ensure the heat transfer to the surrounding external region. This fact shows the good ability of this material as a high thermal conductive material for TES applications.

When the melting starts in the region close to the internal tube, the external thermocouples decreases even more drastically their heating rate due to the fact that all the energy provided by the internal tube is used to melt the surrounding alloy and some of the energy is used to continue with the preheating of the metallic parts of the container. Moreover, as the melting front goes forward, a liquid layer having half thermal conductivity than that of the solid material is formed which limits the heat transfer compared to solid phase. In this sense, at the beginning of the melting process, a small temperature decrease of external thermocouples is observed which might be attributed to thermal inertia of the system.

As the melting front advances to the outer region, the external thermocouples increase their temperature until the melting point, where they remain at constant temperature until the corresponding region is melted.

Concerning the cooling process, the solidification temperature is the same as for the melting, 342 ºC. There is no subcooling effect as it has been previously observed in calorimetric experiments [5, 6]. The reason might be the sample mass influence on the thermal response of the material [16, 17].

The melting time of the PCM at the position of sheath 4 is 81 minutes, while the solidification time is 90 minutes. The temperature difference between inlet temperature and melting point was $\Delta T = 39$ ºC and $\Delta T = 36$ ºC for melting and solidification tests, respectively.

Fig. 3 shows the temperature evolution of external thermocouples (F) of sheaths 1 to 6 in the melting and solidification processes. Sheath 7 is not represented because its values are influenced by the fact of not being dipped into the metal and being in contact with the Ar atmosphere. From the melting curves it can be seen that the melting front advances from top to bottom. On the other hand, the solidification advances in both directions, from top to bottom and vice versa, being the central part (sheaths 3, 4 and 5) the last one to solidify. This might be due to the cooling effect of the two caps at both ends which have a significant exchange surface in contact with the HTF. The total melting and solidification times are given in Table 1.

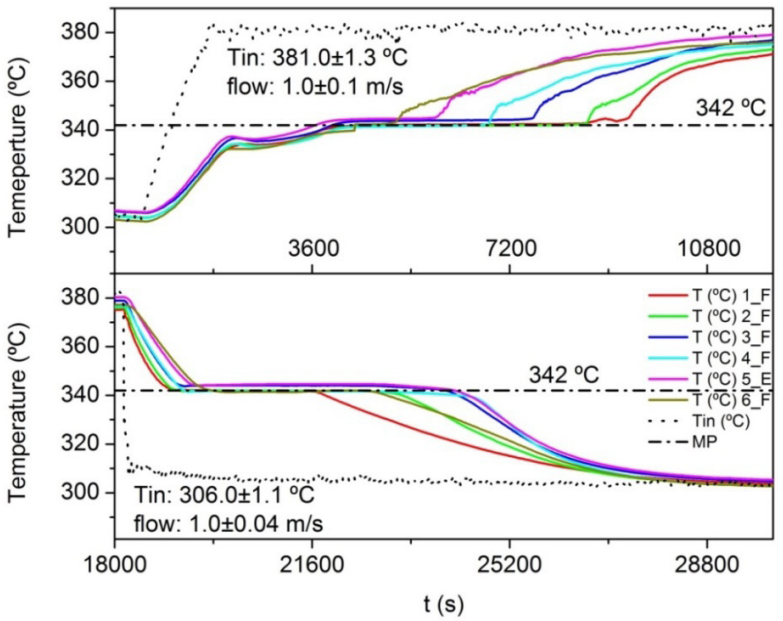

Fig. 3. Temperature evolution of thermocouples F of all sheaths in melting and solidification processes.

Table 1. Melting and solidification times as function of sheath position.

Sheath	1	2	3	4	5	6
Melting time (s)	7270	6510	5860	4870	4200	3400
Solidification time (s)	2710	4150	4830	5420	4940	3360

The total melting time needed to melt all the PCM is 120 minutes while for the solidification it is 90 minutes. Therefore, around 25 % less time is needed to solidify than to melt. This gap together with the difference on the melting and solidification front advances might be attributed to several factors. Among them, the principal ones are the insulation in the bottom part of the unit and the design of the device.

The unit has been fixed on a table with a rock wool blanket of 0.12 m thickness in between both table and bottom flange. It serves as insulation material which has been compressed due to the weight of the unit, and therefore its insulation capacity is expected to be reduced. As a result, the total time for melting is increased and the total time of solidification is reduced.

Concerning the design of the unit, the two caps configuration might contribute to a lower melting rate, especially in the bottom part of the unit where there is direct contact between bottom cap flanges and PCM. In the top part of the unit, Ar gas is in between PCM and top flanges and cap which might be also a reason for the asymmetry of the solidification front.

3.2. Model validation

The explained model has been applied to the particular measurement shown in section 3.1 under the mentioned operation conditions. The obtained results are shown in Fig. 4, where the experimental temperature profiles of sheath 3, chosen as an example, are compared with the results of the modeling.

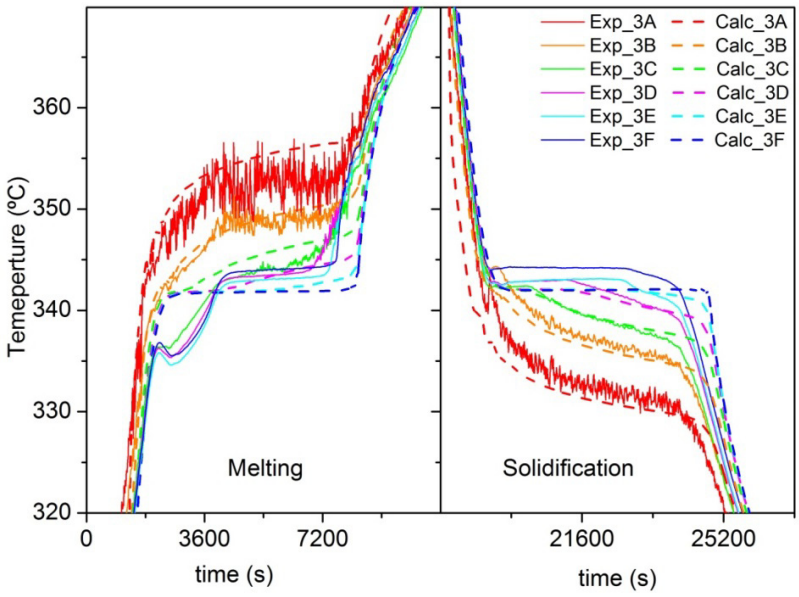

Fig. 4. Charge/discharge (left/right respectively) temperature behavior of the investigated case. Continuous lines correspond to the experimental data. Discontinuous lines represent the calculated radial temperature distribution.

As can be seen, a good fitting is obtained both, in charge and discharge runs. A and B thermocouples show good agreement with the experimental temperatures. The radial temperature distribution between the thermocouples is

also correctly calculated. However, some differences are found. At the beginning of the melting process, the temperature decrease shown by thermocouples C, D, F and E is more pronounced in the experimental data than in the calculated temperatures. As said before, this behavior could be related to the thermal inertia of the experimental TES unit, which might be underestimated in the calculation.

The overall melting/solidification times are successfully determined from the calculation, within a maximum difference of around 10%. The analysis of the data leads to an overall estimated value of the heat transfer coefficient of around h=700 W/m^{2}K.

3.3. Impact of the thermal conductivity on the TES unit

As mentioned before, one of the major benefits of metal alloys used for latent heat storage is their high thermal conductivity. The influence of this parameter on the storage behavior and operation is determinant in order to obtain a fast thermal response unit able to operate at high power values. In this frame, the large thermal conductivity of the proposed material, eutectic Mg-Zn alloy, could imply important advantages in current CSP technologies. However, even in the case of large thermal conductivity materials, the overall heat transfer is determined by conduction/convection mechanisms that need to be modeled in order to determine a realistic influence of the thermal conductivity on the storage system. In this section, a simplified storage unit of the presented design in section 2.2 has been modeled. A simple shell and tube configuration with no caps and no free volume for PCM expansion has been considered. Different thermal conductivity values have been assumed in order to determine its influence on the overall storage device. The rest of the PCM properties have been assumed invariant for all simulations. Concerning the operating parameters of the HTF, the inlet temperature has been set to 400 ºC with a velocity of 3 m/s.

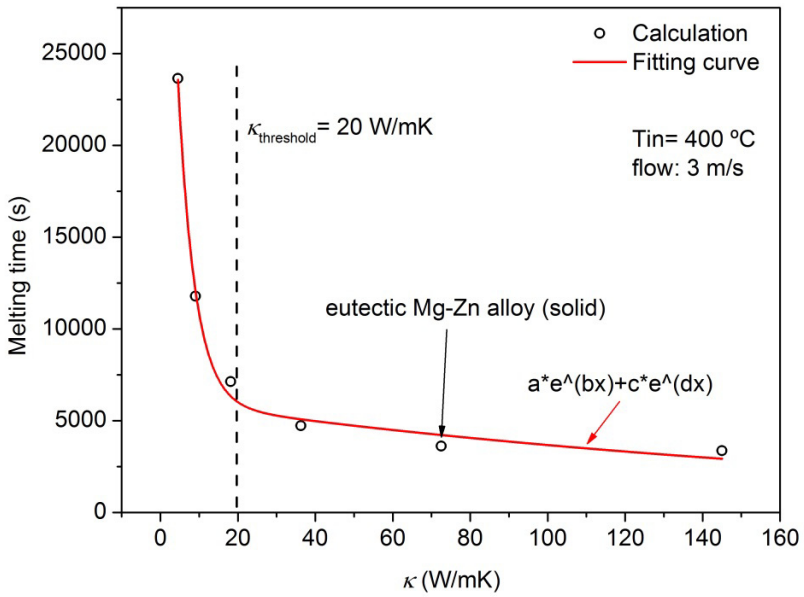

Fig. 5. Influence of the thermal conductivity of the PCM on the melting time. Calculations of the simplified TES design.

As a result, Fig.5 shows the melting time (charging process) as a function of the assumed different thermal conductivities ($\kappa = \kappa^{alloy}/n$, n=0.5, 1, 2, 4, 8 and 16). From Fig.5, it can be clearly seen that around k=20 W/mK there is a conductivity threshold. Under the mentioned HTF conditions, larger conductivity value materials do not represent a big benefit in the storage behavior, as the heat transfer is limited by the HTF convection mechanisms. On the other hand, lower thermal conductivity materials lead to a fast increase of the melting time of the PCM. In this case, the thermal conductivity of the storage material is the limiting issue of the heat transfer. In any case, the competition between convective and conductive mechanisms is the key issue in order to establish this threshold

value of thermal conductivity. In Fig.5, an empirical double exponential function has been used in order to fit the data obtained from the calculation with very good agreement.

In our case, the proposed eutectic Mg-Zn alloy presents a thermal conductivity high enough in both, solid (κ=75 W/mK) and liquid (κ=35 W/mK) phases [6] which guarantees, under the mentioned fluid parameters, that the heat transfer limitation is related to the HTF convection.

3.4. Advantages of Mg-51%Zn as TES

The main advantages of the Mg-51%Zn system arising from the present study are its high thermal conductivity and the quasi constant melting and solidification temperatures.

On the one hand, in the present study, the high thermal conductivity of the eutectic alloy is not the limiting factor for heat transfer, but the heat transfer of the liquid oil inside the pipe. In this regard, if a two-phase fluid is used instead of oil, the system would be charged and discharged faster since the heat transfer of a two-phase fluid (liquid-vapor or vapor-liquid phase changes) is higher. Therefore, experiments such as the one presented by Adinberg et al. [18] would highlight even better the good properties of the metal PCM.

On the other hand, as the melting and solidification temperatures are equal, the differences between charging and discharging HTF conditions are minimized. Concerning direct steam generation application, taking 5 ºC as the temperature difference needed for charging and discharging with respect to melting/solidification temperature, the conditions of the saturated steam needed for charging would be 159 bar at 347 ºC [6] and the produced saturated steam in the discharge process would be 140 bar at 337 ºC. As suggested in [6], the use of this eutectic metal alloy would imply a technological challenge for parabolic trough technology with the need of developing high pressure parabolic trough pipes and corresponding connections. Concerning power tower technology, the challenge would be focused on the development of high pressure central receivers. Apart from CSP applications, this PCM is also proposed as TES material for high pressure or high heat energy steam demanding processes. Nonetheless, due to its high thermal conductivity it could be used for high power heat demanding processes as well.

4. Conclusions

The potential use of eutectic metal alloys as latent heat thermal energy storage has been experimentally investigated by means of heating and cooling tests around the melting point of the phase change material.

There is no subcooling effect as in previous mg scale calorimetric experiments. Melting and solidification temperatures are equal to 342 ºC. Melting and solidification fronts are different due to the combination of different factors such as the used experimental conditions, the design of the prototype, the insulation as well as convection of the liquid melt.

The experimental results have been used to validate a model that has been developed by means of CFD simulations. In addition, with current presented configuration, the limiting factor of the heat transfer comes from the liquid oil inside the pipe and not from the thermal conductivity of the metal PCM. The use of a two-phase fluid as the HTF would highlight even more the properties of the alloy and would allow to study the limitations concerning heat transfer of proposed metal PCM.

Acknowledgements

The authors would like to thank the Department of Industry, Innovation, Commerce and Tourism of the Basque Government for funding Etortek 2011 Energigune'11 grant (IE11-303). The authors would like to express their gratitude to Felix Mendia for his valuable and constructive suggestions and very much appreciate the collaboration of Julian Izaga from IK4-Azterlan and Rafael de Diego from Melfun in the synthesis of the eutectic alloy.

References

[1] D. Laing, C. Bahl, T. Bauer, D. Lehmann, and W. D. Steinmann, “Thermal energy storage for direct steam generation,” Sol. Energy, vol. 85, no. 4, pp. 627–633, Apr. 2011.
[2] D. Laing, T. Bauer, N. Breidenbach, B. Hachmann, and M. Johnson, “Development of high temperature phase-change-material storages,” Appl. Energy, vol. 109, pp. 497–504, Sep. 2013.
[3] H. Michels and R. Pitz-Paal, “Cascaded latent heat storage for parabolic trough solar power plants,” Sol. Energy, vol. 81, no. 6, pp. 829–837, 2007.
[4] V. Zipf, A. Neuhaeuser, D. Willert, P. Nitz, S. Gschwander, and W. Platzer, “High temperature latent heat storage with a screw heat exchanger: Design of prototype,” Appl. Energy, vol. 109, pp. 462–469, Sep. 2013.
[5] J. Rodríguez-Aseguinolaza, P. Blanco-Rodríguez, E. Risueño, M. J. Tello, and S. Doppiu, “Thermodynamic study of the eutectic Mg49–Zn51 alloy used for thermal energy storage,” J. Therm. Anal. Calorim., vol. 117, no. 1, pp. 93–99, Jan. 2014.
[6] P. Blanco-Rodríguez, J. Rodríguez-Aseguinolaza, E. Risueño, and M. Tello, “Thermophysical characterization of Mg–51%Zn eutectic metal alloy: A phase change material for thermal energy storage in direct steam generation applications,” Energy, vol. 72, pp. 414-420, Jun. 2014.
[7] C.R. Swaminathan, V.R. Voller. “A General Enthalpy Method for Modeling Solidification Processes” Metallurgical Transactions B. 23B; pp. 1992-651. 1991.
[8] C.R. Swaminathan, V.R. Voller. “Towards a general numerical scheme for solidification systems” Int J Heat Mass Transfer. Vol 40, 12. pp 2859-2868. 1997
[9] V. R. Voller. "Modeling Solidification Processes". Technical report. Mathematical Modeling of Metals Processing Operations Conference, Palm Desert, CA American Metallurgical Society. 1987
[10] F. Agyenim, N. Hewitt, P. Eames, M. Smyth. “A review of materials, heat transfer and phase change problem formulation for latent heat thermal energy storage systems (LHTESS)” Renewable and Sustainable Energy Reviews 14 615–628. 2010
[11] A.B. Crowley, J.R. Ockendon. “Modelling mushy regions”. Applied Scientific Research 44:1-7 (1987)
[12] V. R. Voller, A. D. Brent and C. Prakash. “Modelling the mushy region in a binary alloy” Appl. Math. Modelling, , Vol. 14, pp. 320-326. 1990
[13] V. R. Voller and C. Prakash. "A Fixed-Grid Numerical Modeling Methodology for Convection-Diffusion Mushy Region Phase-Change Problems". Int. J. Heat Mass Transfer. 30. 1709–1720. 1987.
[14] B.E. Launder and D.B. Spalding. “Lectures in mathematical models of turbulence”. Academic Press, London (England). 1972
[15] B.E. Launder and D.B. Spalding. “The numerical computation of turbulent flows. Comput. Methods Appl. Mech. Eng. Vol. 3, pp. 269-289. 1974.
[16] A. Solé, L. Miró, C. Barreneche, I. Martorell, and L. F. Cabeza, “Review of the T-history method to determine thermophysical properties of phase change materials (PCM),” Renew. Sustain. Energy Rev., vol. 26, pp. 425–436, Oct. 2013.
[17] E. Günther, S. Hiebler, H. Mehling, and R. Redlich, “Enthalpy of Phase Change Materials as a Function of Temperature: Required Accuracy and Suitable Measurement Methods,” Int. J. Thermophys., vol. 30, no. 4, pp. 1257–1269, Aug. 2009.
[18] R. Adinberg, D. Zvegilsky, and M. Epstein, “Heat transfer efficient thermal energy storage for steam generation,” Energy Convers. Manag., vol. 51, no. 1, pp. 9–15, Jan. 2010.